Photocurrent relaxation in pure and Pr-doped a-As_2S_3 films

2004 J. Phys.: Condens. Matter 16 2949

(http://iopscience.iop.org/0953-8984/16/17/021)

INSTITUTE OF PHYSICS PUBLISHING JOURNAL OF PHYSICS: CONDENSED MATTER

J. Phys.: Condens. Matter **16** (2004) 2949–2958 PII: S0953-8984(04)71241-2

Photocurrent relaxation in pure and Pr-doped a-As_2S_3 films

M S Iovu[1], I A Vasiliev[1], E P Colomeico[1], E V Emelianova[2], V I Arkhipov[3] and G J Adriaenssens[2]

[1] Center of Optoelectronics, Strada Academiei 1, MD-2028, Chisinau, Republic of Moldova
[2] Laboratorium voor Halfgeleiderfysica, University of Leuven, B-3001 Leuven, Belgium
[3] IMEC, Kapeldreef 75, B-3001 Leuven, Belgium

Received 30 October 2003
Published 16 April 2004
Online at stacks.iop.org/JPhysCM/16/2949
DOI: 10.1088/0953-8984/16/17/021

Abstract

Photocurrent relaxation was investigated in pure and Pr-doped amorphous As_2S_3 films after constant illumination had been switched off. It is shown that, in the temperature range from 290 to 370 K and for the time interval 0.5–150 s, the photocurrent relaxation might be approximated as an algebraic function. An analytic model of the recombination-controlled photocurrent decay in amorphous semiconductors is formulated. For the As_2S_3 samples with Pr impurity, the relaxation rate is lower and the form of the decay profile varies only lightly in comparison with non-doped samples. The results are discussed in terms of the band tails and deep acceptor-like centres present in a-As_2S_3 films.

1. Introduction

It is well known that metal impurities affect optical, photoelectric and transport properties of thermally evaporated amorphous chalcogenide films [1, 2]. Recently, the influence of metal impurities on transient characteristics of photoconductivity and optical absorption was studied in [3–5]. These impurities are supposed to create new defect states and/or change the short- and medium-range order in the film. The photocurrent relaxation in pristine amorphous As_2Se_3 films and AsSe films doped with tin was interpreted in terms of the trap-controlled recombination with a broad quasi-continuous distribution of localized states [6–8].

The relaxation of photocurrent in a-As_2S_3 films has been investigated to a lesser degree: the low electrical conductivity and polarization at the contacts essentially complicate both measurements of relaxation and the data analysis in this material. The interest in As_2S_3 films doped by rare earth ions (such as praseodymium) is connected with new applications of these films in optoelectronics as laser light sources, operating at a wavelength of 1.3 μm and fully built-in into the integrated circuits of optical telecommunication systems. In the present paper,

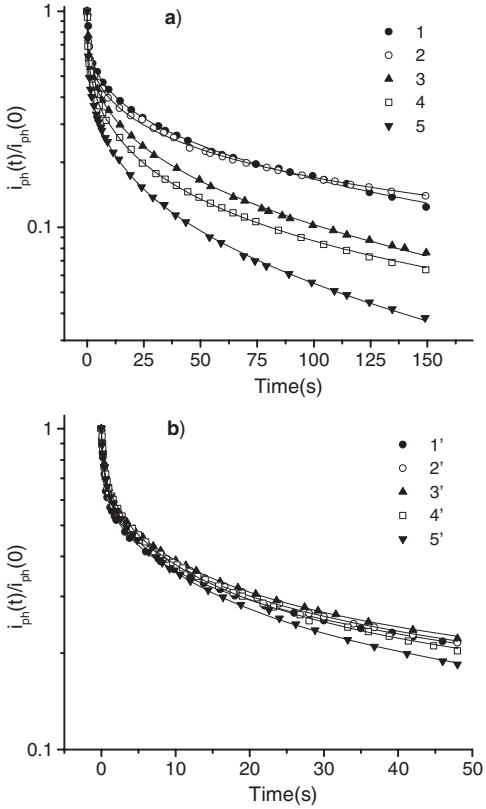

Figure 1. Time dependences of the normalized photocurrent $i_{ph}(t)/i_{ph}(0)$ for As_2S_3 (a) and As_2S_3:Pr (b) samples measured at 318 K (a) and 322 K (b) at the following light intensities F (in photon cm^{-2} s^{-1}): 1—1.3×10^{12}; 1′—2.6×10^{12}; 2, 2′—6.5×10^{12}; 3, 3′—1.69×10^{13}; 4, 4′—2.8×10^{13}; 5, 5′—6.3×10^{13}. The curves represent fitted stretched-exponential functions.

we report an experimental study of the effects of Pr doping and temperature on the long-term photocurrent relaxation in thermally evaporated amorphous As_2S_3 films. We further examine the possibility of extracting density-of-states (DOS) information from the relaxation curves.

2. Experimental results

Praseodymium was introduced in amounts of 0.05–0.25 at.% into As_2S_3 during standard thermal synthesis of the material. Thin films ($L = 3$–4 μm) were obtained by flash evaporation in vacuum on glass substrates held at $T = 120\,^{\circ}$C. The films were sandwiched between two sputtered Al electrodes ($\sim$0.56 cm^2), of which the top one was semitransparent. The photocurrent was induced through the top electrode by a monochromatic light pulse ($\lambda = 0.49$ μm, $\Delta\lambda = 20$ nm) from the tungsten–halogen lamp of a SPM-2 spectrophotometer. The pulse duration was about 25 s with a light intensity of 10^{12}–10^{14} photon cm^{-2} s^{-1}. The photocurrent was led through an electrometric amplifier and was registered by a two-coordinate recorder. A constant voltage of about 4.0 V was applied to the top illuminated electrode.

Figure 1 shows the decay of photoconductivity after the cessation of light excitation in films of As_2S_3 (a) and As_2S_3:Pr (b), measured at the temperature $T = 318$ (322) K and at light intensities F, ranging from 1.3×10^{12} up to 6.3×10^{13} photon cm^{-2} s^{-1}. All the curves were normalized to the photocurrent at the moment when the light was switched off. One can see that

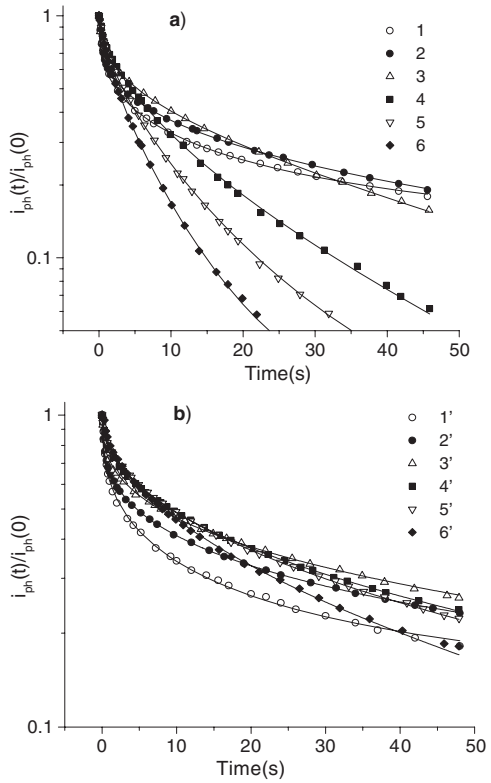

Figure 2. Time dependences of the normalized photocurrent $i_{ph}(t)/i_{ph}(0)$ for samples As_2S_3 (a) and As_2S_3:Pr (b), measured after cessation of optical excitation with intensity $F = 6.5 \times 10^{12}$ photon cm^{-2} s^{-1}, at various temperatures T (in K): 1, 1′—308 (310.5); 2, 2′—320 (322); 3, 3′—331 (333); 4, 4′—342 (344); 5, 5′—348 (349.5); 6, 6′—353 (355). Full curves show the fitting curves.

introduction of Pr impurity changes the decay curves significantly. This distinction is strongest at high light intensities ($F > 1.7 \times 10^{13}$ photon cm^{-2} s^{-1}) and at longer decay times ($t > 2$ s). The photocurrent decay rate sharply increases with increasing light intensity in As_2S_3 films whereas the shape of the photocurrent decay curves do not vary much in the As_2S_3:Pr samples. The normalized photocurrent in the doped samples follows the curve measured in the undoped sample at the lower light intensity, $F < 1.7 \times 10^{13}$ photon cm^{-2} s^{-1}.

The temperature effect on the photocurrent decay kinetics in As_2S_3 and As_2S_3:Pr films is more complex—see figure 2. The data, plotted in this figure, indicate a weak dependence of the photocurrent decay on the temperature in both doped and undoped samples in the low temperature range $T < 340$ K. In this temperature range and at longer times, the value of the photocurrent remains essentially unchanged (curves 1, 2, 3 and 1′, 2′, 3′, respectively). Above $T = 340$ K, an appreciable change of the decay rate and of the curve shape accompanied by a sharp reduction of the photocurrent was observed in the undoped samples. The praseodymium-doped samples do not reveal similar behaviour: the relative photocurrent still slowly varies in time such that its value drops only by a factor of 3–5 after 50 s of relaxation, irrespective of the temperature.

The lines through the data points in figures 1 and 2 represent stretched exponential functions of the type $I_{ph}(t) = I_{ph}(0) \exp[-(t/\tau)^{\alpha}]$, where τ is a characteristic decay time constant and $0 < \alpha < 1$ is the stretching exponent. Table 1 shows fitted values for those

Table 1. Comparison of system parameters and photoconductivity results from pure and Pr-modified As_2S_3 films, showing measurement temperature T, initial photocurrent $I_{ph}(0)$, dark current I_{dark}, dark current activation energy E_σ and fitting parameters α and τ of the stretched exponential function.

Pr (at.%)	T (K)	$I_{ph}(0)$ (pA)	I_{dark} (pA)	E_σ (eV)	α	τ (s)
0.00	326	220	1.5		0.37	10.1
	342	650	10		0.59	7.8
	353	1030	30	1.12	0.71	4.0
	364	1420	110		0.81	2.2
0.15	322	36	2		0.32 (0.34)	14.5
	339	97	8		0.40 (0.41)	22.7
	355	270	30	1.16	0.52 (0.48)	16.2
	366	435	76		0.62 (0.47)	9.7

parameters at four temperatures above 320 K, together with reference values for the measured dark currents and photocurrents in pure and Pr-doped As_2S_3. In this temperature range the stretching exponent α increases steeply to values above 0.8 at 360 K in undoped, and above 0.6 in doped, As_2S_3 samples, while staying around 0.3–0.4 at lower temperatures. Analogously, the increase in the decay time constant with decreasing temperature also levels off at lower temperatures.

While a stretched-exponential expression has been derived earlier for photocurrent relaxation in amorphous semiconductors with exponential band tails $g(E) \propto \exp(-E/E_0)$ [9], it was subsequently shown to be valid only for a limited range of the system parameters [10]. Specifically, the relaxation should be dominated by a multiple trapping process rather than by recombination and the temperature should be below the characteristic temperature $T_0 = E_0/k$ of the tail. The stretching exponent should correspond to $\alpha = T/T_0$ in that case, which contrasts with the experimental results outlined above. The next section, therefore, re-examines the general problem of photocurrent relaxation from a steady state.

3. Trap-controlled relaxation of photocurrent

Relaxation of photogenerated charge carriers, i.e. relaxation of photoconductivity, in amorphous semiconductors occurs due to either mono- or bimolecular recombination of charge carriers. In materials with high densities of localized states, the absolute majority of charges are localized at any given time. Recombination of localized carriers is difficult because it requires tunnelling while bimolecular recombination of a pair of free carriers is highly improbable. Therefore, recombination occurs only if a free carrier encounters either a recombination centre (monomolecular recombination, MR) or a carrier of the opposite sign (bimolecular recombination, BR). Since the characteristic depth of electron traps in chalcogenide glasses is much larger than that of hole traps, the most probable is recombination of a free hole. Under the condition of quasi-neutrality the densities of photogenerated electrons and holes are equal to each other and the recombination equation takes the form

$$\frac{\mathrm{d}p(t)}{\mathrm{d}t} = -\frac{p_c(t)}{\tau_r} - Rp_c(t)p(t), \tag{1}$$

where p_c is the density of free holes, p is the total density of holes (and hence also of trapped electrons, i.e. the recombination centre density), τ_r is the monomolecular recombination time and R is the bimolecular recombination constant. In general, one must account for contributions

of both free and localized carriers into the total carrier density. However, in amorphous materials, most carriers occupy localized states and the contribution of free carriers into the total density is negligibly small. Therefore, the equation for the total density of holes can be written as

$$p(t) = \int_0^\infty \mathrm{d}E\, \rho(E,t), \tag{2}$$

where E is the energy of a localized state and ρ is the energy distribution of the density of localized holes. The latter is controlled by carrier trapping and release rates within the manifold of quasi-continuously distributed localized states:

$$\frac{\partial \rho(E,t)}{\partial t} = \frac{g(E) - \rho(E,t)}{\tau_0 N_\mathrm{t}} p_\mathrm{c}(t) - \nu_0 \exp\left(-\frac{E}{kT}\right)\rho(E,t), \tag{3}$$

where $g(E)$ is the density-of-states (DOS) distribution, N_t is the total, energy-integrated, density of localized states, τ_0 is the free carrier lifetime with respect to trapping, ν_0 is the attempt-to-release frequency and k is the Boltzmann constant.

In the present paper, we consider slow relaxations of the photocurrent starting from its steady-state level. Under these conditions, the initial energy distribution of localized charge carriers, $\rho_0(E) = \rho(E,0)$, is described by the Fermi–Dirac function as

$$\rho_0(E) = \frac{g(E)}{1 + \exp\left(-\frac{E-E_\mathrm{F}}{kT}\right)}, \tag{4}$$

where E_F is the energy of the quasi-Fermi level established during illumination of the sample. Long-time relaxation of photoconductivity requires the release of carriers trapped by localized states above the quasi-Fermi level that have been fully occupied during photoexcitation and, therefore, the initial energy distribution of carriers can be simplified as

$$\rho_0(E) = g(E), \qquad E > E_\mathrm{F}. \tag{5}$$

In order to calculate the relaxation rate one first needs to identify the rate-limiting step in the relaxation process. The carrier release rate exponentially decreases with increasing energy of localized states and, therefore, the first carrier release from a localized state above the quasi-Fermi level is an obvious candidate for the rate-limiting step. This is the case if the released carrier recombines before it could be retrapped by an equally deep or deeper localized state. It may be noted that the initial quasi-Fermi level for holes will only mark that demarcation at the onset of the relaxation; it will be supplanted by an increasingly deeper-lying release level as relaxation progresses. The recombination rate is given either by $p_\mathrm{c}/\tau_\mathrm{r}$ for the MR process or by the $Rp_\mathrm{c}p$ product when BR dominates, while the rate of retrapping by the deep states is $(1/\tau_0)(N_\mathrm{d}/N_\mathrm{t})p_\mathrm{c}$, where N_d is the density of vacant deep localized states. It should be noted that the inverse product of the free carrier lifetime and the total density of localized states is simply the average capture coefficient: $c_0 = 1/N_\mathrm{t}\tau_0$. Since most deep states have been occupied by carriers prior to the onset of photocurrent relaxation the density of vacant deep traps is much smaller than the carrier density at any time of relaxation: $N_\mathrm{d} \ll p$. Therefore, recombination is much faster than carrier release from deep traps unless the recombination constant is much smaller than the capture cross section, which is fairly unrealistic because recombination is facilitated by the Coulomb attraction of carriers while empty localized states are neutral. Under these conditions, the total carrier density is fully controlled by the carrier release rate, which leads to the following expression for the function $p(t)$ [11]:

$$p(t) = \int_0^\infty \mathrm{d}E\, \exp\left[-\nu_0 t \exp\left(-\frac{E}{kT}\right)\right] g(E) \cong \int_{kT\ln(\nu_0 t)}^\infty \mathrm{d}E\, g(E). \tag{6}$$

In the simplest case of MR, substituting equation (6) into (1) yields the following expression for the time dependence of the photocurrent density i_{ph}:

$$i_{ph}(t) = e\mu_c F\tau_r \frac{kT}{t} g(kT \ln \nu_0 t), \tag{7a}$$

where e is the elementary charge, μ_c is the free carrier mobility and F is the applied field. In the BR case, this relationship takes the form

$$i_{ph}(t) = e\mu_c F \frac{kT}{Rt}\left[\int_{kT\ln(\nu_0 t)}^{\infty} \mathrm{d}E\, g(E)\right]^{-1} g(kT \ln \nu t). \tag{7b}$$

Similar to the signals in transient photoconductivity [12] or post-transit current measured in time-of-flight (TOF) experiments [13], the photocurrent relaxation rate is governed by the DOS distribution. However, at variance with the post-transit TOF current analysis, the time dependence of the photocurrent is *directly* related to the DOS function only in the MR case, as one can see from equations (7*a*) and (7*b*). In fact, the experimentally observed time dependence of the photocurrent may be practically insensitive to the DOS distribution when BR dominates. For instance, the band-tail DOS distributions are often approximated by exponential functions of energy as

$$g(E) = \frac{N_t}{E_0} \exp\left(-\frac{E}{E_0}\right), \tag{8}$$

where E_0 is the characteristic energy of the distribution. For this DOS distribution equation (7*b*) yields the photocurrent

$$i_{ph}(t) = e\mu_c F p_c(t) = e\mu_c F \frac{kT}{E_0}\frac{1}{t}, \tag{9}$$

whose time dependence is universal irrespective of the DOS width. The only remnant of the DOS function in equation (9) is the coefficient kT/E_0. Nevertheless, for a DOS that is not as featureless as that of equation (8), one may expect that some characteristic features of the photocurrent relaxation curve reflect that non-monotonic DOS.

In figure 3, some of the experimental data of figure 2 are used to construct $I_{ph}(t) \times t$ versus $kT\ln(\nu t)$ diagrams in analogy with those that would represent the underlying DOS in the case of a TOF post-transit photocurrent analysis (PTPA). Differences are observed between the curves for pure and Pr-modified As_2S_3, but in both instances data sets generated at different temperatures exhibit the mutual agreement that they must have if they are to represent the DOS. An analysis in terms of equations (7*a*) or (7*b*) becomes feasible if a superposition of an exponential band-tail and a Gaussian distribution of deep traps is used for $g(E)$. Calculated values based on the introduction of

$$g(E) = \frac{N_t}{E_0}\exp\left(-\frac{E}{E_0}\right) + \frac{N_d}{\sqrt{2\pi}\sigma}\exp\left[-\frac{(E-E_d)^2}{2\sigma^2}\right], \tag{10}$$

with N_d and E_d being the density and average energy of deep traps and σ being the width of the trap distribution, in either equation (7*a*) or (7*b*) have been included in figures 3(a) and (b), respectively.

The shape of the theoretical curves in figure 3(a), with their well-defined maximum, is characteristic of the combination of the DOS of equation (10) and the monomolecular recombination process. Taken at face value, the good agreement between the measured and calculated $I_{ph}(t) \times t$ curves would indicate the presence in the As_2S_3 DOS of a defect band located ~0.9 eV above the valence band. However, the measured values of the dark and photocurrents, displayed in table 1, show $I_{ph}(0) \gg I_{dark}$ for all temperatures and, consequently, that bimolecular recombination should dominate. In other words, since the E_V + 0.9 eV

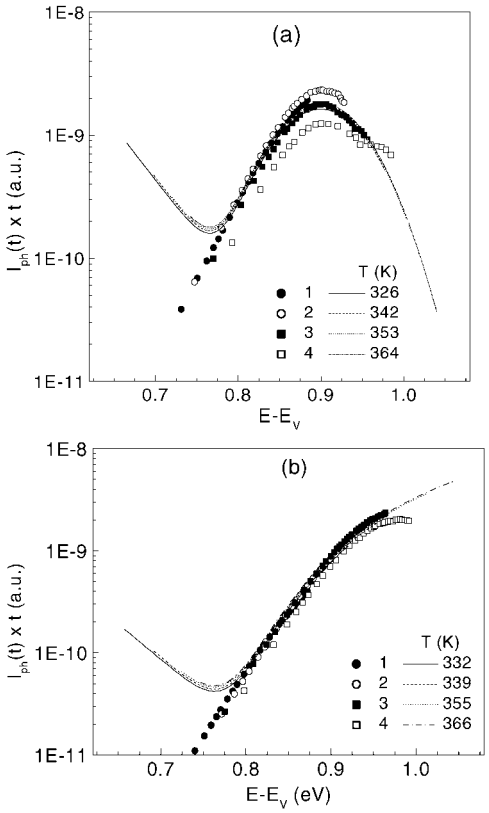

Figure 3. Apparent DOS distributions calculated on the basis of the experimental data (symbols), together with fitted curves (lines) based on equations (7) and the DOS of equation (10). (a) Pure As_2S_3, using the MR equation (7*a*) and $E_d = 0.90$ eV, $N_d = 3.5 \times 10^{16}$ cm^{-3}, $\sigma = 0.05$ eV, $\tau_r = 10^{-4}$ s, $\nu = 10^{12}$ s^{-1}, $\mu_c = 10^{-5}$ cm^2 V^{-1} s^{-1}, $F = 10^4$ V cm^{-1}, $E_0 = 0.05$ eV, $N_t = 10^{21}$ cm^{-3}, sample area 0.56 cm^2. (b) As_2S_3:Pr with BR according to (7*b*), $E_d = 0.96$ eV, $N_d = 5.0 \times 10^{17}$ cm^{-3}, $\sigma = 0.066$ eV, $R = 10^{-12}$ cm^{-3} s^{-1} and the remaining parameters as above.

position of the defect band was obtained on the basis of MR rather than BR, it cannot be trusted. This point will be further discussed in the next section. The calculated curves of figure 3(b) in turn are characteristic for the bimolecular process where, as noted above, details of the DOS will not be correctly resolved. Nevertheless, from the use of the BR formalism to analyse the data from the Pr-doped samples and from the close agreement between measured and calculated curves, it could be concluded that a Gaussian defect band, some ∼0.96 eV above E_V, is indeed present in the material.

The time dependence of the photocurrent, calculated with equation (7*b*) on the basis of the DOS of equation (10) with the parameters used for figure 3(b), is plotted in figure 4 for different temperatures. The Gaussian peak of deep traps is revealed by the departure from the initial power-law decay of the photocurrent. The departure occurs at increasingly later times for increasingly lower temperatures, but always very early in the timeframe of our experimental relaxation curves. Also shown in figure 4 (full curves) are fits to the calculated curves with the stretched exponential function that was originally used to describe the relaxation data. The values for the stretching parameter α that resulted from these fits have been added in parentheses to table 1. Satisfactory agreement between the two sets of α values supports the use of the BR formalism to interpret the As_2S_3:Pr relaxation curves.

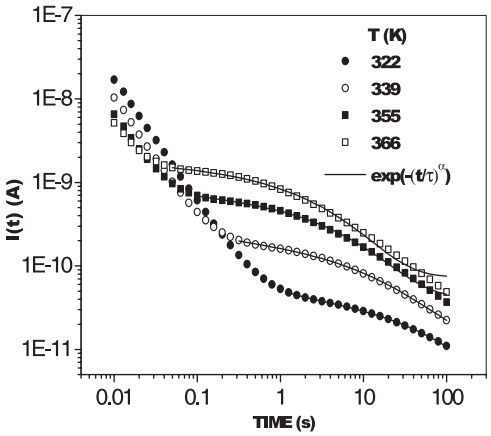

Figure 4. Calculated photocurrent relaxation curves (symbols) controlled by bimolecular recombination of charge carriers (equation (7*b*)) at different temperatures as in figure 3(b), together with fitted stretched exponential functions (lines).

4. Discussion

The non-exponential relaxation of photoconductivity (figures 1 and 2) is typical for the majority of amorphous semiconductors and is usually attributed to a wide spectrum of localized states in a mobility gap [6, 7]. It is generally assumed that, after light cessation, the photocurrent decays due to the capture of non-equilibrium charge carriers (holes) by band tail localized states and, later on, due to recombination. This process is obviously responsible for the observed photocurrent relaxation in the As_2S_3 and As_2S_3:Pr films. From the fact that the data can be fitted with a stretched exponential function rather than the power law predicted by the recombination analysis of section 3, one might conclude that multiple-trapping relaxation is observed in an exponential distribution of states with, according to [10], a characteristic temperature T_0 larger than the highest temperature used in this study, i.e. 370 K. Considering that the valence band tail in As_2Se_3 was found to have $T_0 \approx 550$ K [14], this is not unreasonable.

However, the observed temperature dependence of the stretching exponent α cannot be explained by relaxation in a purely exponential distribution of localized states, where it would have to follow $\alpha = T/T_0$. Of course, both native charged defects and impurities also contribute to the DOS distribution in chalcogenide glasses [15, 16]. Due to the positional disorder, the appropriate defect levels are also quasi-continuously distributed in energy and a Gaussian function gives a realistic description of this distribution [17]. Therefore, the results obtained in the previous section with the combination of an exponential tail and a Gaussian defect band do have merit. At the same time though, some problems remain outstanding. That the pure-As_2S_3 data could be fitted best with the MR equation (7*a*) is one such problem. In principle, it should also be possible to adjust the DOS parameters and use BR to fit a non-monotonic $I \times t$ curve, as can be learned from the 350 K curve of figure 5, but then the resolved maximum would not reflect the actual position of the defect band and the parameters would not necessarily be realistic. A further experimental observation that reflects on the choice for a MR or BR model is the Lux–Ampère characteristic of the photocurrent, $I_{\rm ph} \propto ({\rm Int})^{\gamma}$, where Int stands for the light intensity. In the standard analysis of photoconductivity in chalcogenide glasses [18], the exponent γ takes the value 1 with MR and 0.5 for BR. For the photocurrents reported in this study, the Lux–Ampère exponent was, respectively, 0.9 and 1.1 for the pure and doped samples. In other words, even though the current ratio $I_{\rm ph}(0)/I_{\rm dark} \gg 1$ suggests BR, the exponent γ

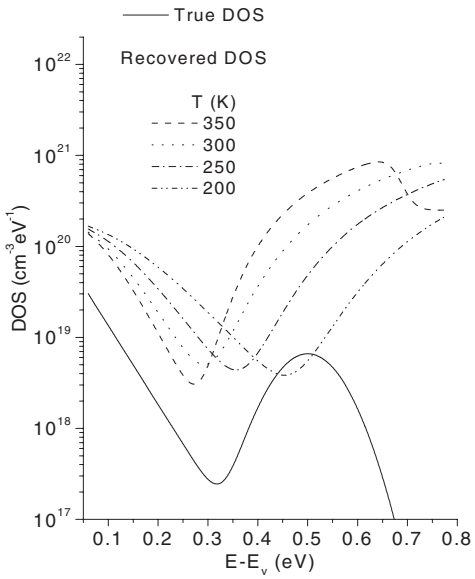

Figure 5. The apparent DOS distributions calculated on the basis of equations (7*b*) and (10) with $\nu = 10^{11}$ s^{-1}, $N_t = 10^{20}$ cm^{-3}, $E_0 = 0.05$ eV, $N_d = 10^{18}$ cm^{-3}, $E_d = 0.5$ eV and $\sigma = 0.06$ eV for the indicated temperatures, together with the original DOS that was used to calculate those curves.

points to a MR process. A combination of causes may lie behind these conflicting signals: in highly disordered systems like a-As_2S_3, 25 s of illumination may still not be sufficiently long for an initial stationary state to be fully attained, while during the subsequent relaxation process not just recombination but also carrier thermalization in the distribution of localized states will play a role.

The characteristics of the slow photocurrent decay, as observed in the present study in both As_2S_3 and, especially, in As_2S_3:Pr amorphous films, indicate that capture of non-equilibrium holes by both tail states and deep acceptor-like centres must be involved. While the density of these centres will be of the order of the native defect concentration ($\sim 10^{17}$ cm^{-3}) in pure As_2S_3, the considerably higher concentration of Pr^{3+} ions in the doped material will result in a much higher compensating density of acceptor-like states. Apart from its influence on charged defects, Pr will also induce further states in the gap by virtue of the lattice distortion caused by its large ionic radius. Evidence for such lattice distortion is provided by the reduction of photoinduced anisotropy upon Pr introduction in chalcogenide glasses [19] and by the measured broadening of the Urbach tail in As_2S_3 doped with 0.1% Dy, a comparable rare-earth element [20]. In the latter case the additional defect density was estimated as 10^{17} cm^{-3}. The increased density N_d of the Gaussian peak that is required to fit the As_2S_3:Pr data with respect to the As_2S_3 results (see figure 3) follows the same pattern.

This difference in localized state distributions in pristine and Pr-doped samples allows us to explain the light intensity dependence of relaxation curves shown in figures 1(a) and (b). If the intensity of light is low, the concentration of non-equilibrium charge carriers is insufficient for saturation of the deep centres and the rate of photocurrent decay should be the same for both samples. Curves 1–4 in figures 1 and 2 do reveal no light intensity dependence of the photocurrent relaxation up to the values of light intensity of $F = 10^{13}$ photon cm^{-2} s^{-1}.

Since the direct PTPA approach is only applicable to photocurrent relaxation controlled by monomolecular recombination, a condition that is seriously in doubt for the data in this

study, the identification of the precise DOS distribution turns out to be a complex problem that can be resolved only on the basis of a recurrent analysis. However, given the notorious problems in this type of analysis with the reliability of the recovered DOS distribution, due to a high sensitivity to experimental error margins and noise, no attempt at further iterative resolution was made. One observation that can be made in connection with the BR-resolved *apparent* DOS distribution is that it reveals a continuously increasing density of deep traps towards the Fermi level. DOS functions deduced from a true TOF PTPA often do show a similar rise near mid-gap, which may signify a spurious influence of either the dark current or bimolecular recombination at longer times in the photocurrent relaxation.

5. Conclusions

As testified by the light intensity and temperature dependences of the photocurrent relaxation rate, the kinetics of this process is controlled by both exponential band tail localized states and a distribution of deep traps in both pristine and praseodymium-doped As_2S_3. The energy range of the deep state distribution is estimated as ∼0.5–1.0 eV. The observed effect of the praseodymium doping is an increase in the density of deep traps, in good agreement with published data.

Although the post-transit photocurrent analysis is fully applicable to the analysis of the photocurrent relaxation controlled by monomolecular carrier recombination, it fails to yield the DOS distribution from the data on photocurrent decay controlled by bimolecular recombination. An attempt to apply this method would lead to a strong overestimate of the density of deep traps with activation energies approaching the Fermi energy.

Acknowledgment

INTAS (grant 99–01229) is acknowledged for support of this work.

References

[1] Kolomiets B T and Averyanov V L 1985 *Physics of Disordered Materials* ed D Adler, H Fritzsche and S R Ovshinsky (New York: Plenum) p 663
[2] Kalmykova N P, Mazets T F, Smorgonskaya E A and Tsendin K D 1989 *Fiz. Tekh. Poluprov.* **28** 297
[3] Iovu M S, Shutov S D and Toth L 1997 *Phys. Status Solidi* b **195** 710
[4] Iovu M S, Shutov S D and Popescu M 2002 *J. Non-Cryst. Solids* **299** 924
[5] Iovu M, Shutov S, Rebeja S and Kolomeiko E 1998 *Phys. Status Solidi* b **206** 583
[6] Andriesh A M, Arkhipov V I, Iovu M S, Rudenko A I and Shutov S D 1983 *Solid State Commun.* **48** 1041
[7] Arkhipov V I, Iovu M S, Rudenko A I and Shutov S D 1985 *Fiz. Tekh. Poluprov.* **19** 101
[8] Iovu M S, Shutov S D, Arkhipov V I and Adriaenssens G J 2002 *J. Non-Cryst. Solids* **299** 1008
[9] Adriaenssens G J, Baranovskii S D, Fuhs W, Jansen J and Öktü Ö 1995 *Phys. Rev.* B **51** 9661
[10] Cordes H, Bauer G H and Brüggemann R 1998 *Phys. Rev.* B **58** 16160
[11] Arkhipov V I and Rudenko A I 1982 *Phil. Mag.* B **45** 189
[12] Emelianova E V, Song H-Z, Arkhipov V I and Adriaenssens G J 2000 *J. Non-Cryst. Solids* **266** 884
[13] Seynhaeve G F, Barclay R P, Adriaenssens G J and Marshall J M 1989 *Phys. Rev.* B **39** 10196
[14] Monroe D and Kastner M A 1986 *Phys. Rev.* B **33** 8881
[15] Street R A and Mott N F 1975 *Phys. Rev. Lett.* **35** 1293
[16] Kastner M and Fritzsche H 1978 *Phil. Mag.* B **37** 199
[17] Arkhipov V I, Kazakova L P, Lebedev E A and Rudenko A I 1987 *Fiz. Tekh. Poluprov.* **21** 724
[18] Mott N F and Davis E A 1979 *Electronic Processes in Non-Crystalline Materials* 2nd edn (Oxford: Clarendon)
[19] Seddon A B, Furniss D, Iovu M S, Shutov S D, Syrbu N N, Andriesh A M, Hertogen P and Adriaenssens G J 2003 *J. Optoelectron. Adv. Mater.* **5** 1107
[20] Iovu M S, Shutov S D, Andriesh A M, Kamitsos E I, Varsemis C P E, Furniss D, Seddon A B and Popescu M 2001 *J. Optoelectron. Adv. Mater.* **3** 443